CLUTTER REJECTION USING RANGE-RECURSIVE SPACE-TIME ADAPTIVE PROCESSING (STAP) ALGORITHMS IN NON SIDELOOKING CONFIGURATION

Sophie BEAU and Sylvie MARCOS

Laboratoire des Signaux et Systèmes, CNRS, Supelec
3, rue Joliot-Curie, 91192 Gif-sur-Yvette cedex
phone: +33 [0]1 69851746, fax: +33 [0]1 69851765,
e-mail: fourcade@lss.supelec.fr , marcos@lss.supelec.fr

ABSTRACT

In this paper, we address the issue of ground clutter rejection for the detection of slowly moving targets in a non sidelooking (NSL) array configuration airborne radar. The classical space-time adaptive processing (STAP) such as the SMI or the eigencanceller-based methods are computationally costly and require the estimation of the clutter covariance matrix from secondary data. However in monostatic STAP airborne radar, the main consequence of the inclination of the array is the range dependency of the clutter covariance matrix. Several compensation methods exist but they are computationally complex or require the knowledge of the radar parameters. We here investigate the use of range recursive subspace-based algorithms of linear complexity inspired by existing time recursive array processing and we show that they are able to track the range dependency (non stationarity) of the data.

1. INTRODUCTION

A main issue in airborne radar signal processing is the detection and the tracking of slowly moving targets. Indeed, a low velocity target can be masked by the ground clutter generated by the radar platform speed. Space-time adaptive processing (STAP) may improve this detection by rejecting the ground clutter [1]. The conventional fully adaptive STAP known as the sample matrix inversion (SMI) method as well as the subspace-based eigencanceller are not actually used in practice because of their prohibitive computational cost which prevents their real-time implementation [1]. That is why we here focus on adaptive algorithms which may recursively compute a subspace-based STAP rejector directly from the data with a linear complexity. We here consider the context of a monostatic airborne radar in a non sidelooking configuration. The radar antenna is an uniformly spaced linear array antenna composed of N half wavelength spaced elements which is not aligned with the platform velocity vector and transmits a train of M pulses at a constant pulse repetition frequency (PRF). L samples for each pulse repetition interval (PRI) are collected to cover a range interval. A data cube is constructed with bidimensional (sensor, pulse) snapshots at different ranges and is exploited to calculate with a STAP algorithm the weights of the clutter rejection filter. In a sidelooking configuration, the clutter covariance matrix involved in conventional STAP algorithms is range independent and can then be estimated from the secondary range cells. In a non sidelooking configuration, the velocity misalignment changes the nature of the clutter and consequently the techniques of rejection. Several compensation methods exist (see [2] and the reference in it) but they are computationally complex or require the knowledge of the radar parameters. We here propose, as an alternative, to use range recursive subspace-based algorithms of linear complexity and we show that they are capable of tracking the range dependency of the data. Next section describes the signal model, the non sidelooking configuration and its consequences. In section 3, the investigated range recursive algorithms are presented. Simulation results and a discussion are given in section 4. Concluding remarks are in section 5.

2. SIGNAL MODEL AND NON SIDELOOKING CONFIGURATION

2.1 Signal Model

A space time snapshot at range k in the presence of a target is given by

$$\mathbf{x}(k) = \alpha_t \mathbf{v}_t + \mathbf{x}_{i+n}(k)$$

where α_t is the unknown target amplitude, $\mathbf{v}_t$ is the target steering vector and $\mathbf{x}_{i+n}(k)$ is the interference plus noise signal vector. Here the Doppler is supposed to be unambiguous. The ground clutter is here the only interference component and it is supposed unambiguous in range. The target steering vector is defined by

$$\mathbf{v}_t = \mathbf{b}(\varpi_t) \otimes \mathbf{a}(\vartheta_t) \tag{1}$$

where

$$\mathbf{b}(\varpi_t) = [1; e^{j2\pi\varpi_t}; \ldots; e^{j(M-1)2\pi\varpi_t}] \tag{2}$$

is the temporal steering vector with ϖ_t the target spatial frequency and

$$\mathbf{a}(\vartheta_t) = [1; e^{j2\pi\vartheta_t}; \ldots; e^{j(N-1)2\pi\vartheta_t}] \tag{3}$$

is the spatial steering vector with ϑ_t the target Doppler frequency. The interference plus noise $\mathbf{x}_{i+n} = \mathbf{x}_c + \mathbf{x}_n$ is composed of a noise vector $\mathbf{x}_n$ supposed to be spatially and temporally white and a ground clutter component

$$\mathbf{x}_c = \sum_{i=1}^{N_c} \alpha_i \mathbf{v}_c(\vartheta_i, \varpi_i)$$

α_i is the amplitude of the ith azimuth clutter patch and $\mathbf{v}_c$ is defined in the same way as (1), (2) and (3) with ϑ_i and ϖ_i being the Doppler and spatial frequencies respectively. The optimum weights of the interference plus noise rejection filter is given by [1],

$$\mathbf{w}_{opt} = \kappa \mathbf{R}_{i+n}^{-1} \cdot \mathbf{v}_t$$

κ is a scalar of normalization and $\mathbf{R}_{i+n} = E\left\{\mathbf{x}_{i+n}\mathbf{x}_{i+n}^H\right\} = \mathbf{R_c} + \mathbf{R_n}$ is the interference plus noise covariance matrix where $\mathbf{R_c} = E\left\{\mathbf{x}_c\mathbf{x}_c^H\right\}$ and $\mathbf{R_n} = \sigma^2\mathbf{I}$ are the clutter and the noise space-time covariance matrices, respectively.

In practice $\mathbf{R}_{i+n}$ is unknown and must be estimated from the snapshots. The well-known SMI (sample matrix inversion) consists in an estimation of the matrix by averaging over the secondary range cells,

$$\widehat{\mathbf{R}}_{i+n}(k) = \frac{1}{K} \sum_{l=1, l\neq k}^{N} \mathbf{x}_l \mathbf{x}_l^H \tag{4}$$

where k is the test range cell and K is the number of secondary range cells. The SMI weight vector is then

$$\mathbf{w}_{smi} = \kappa \widehat{\mathbf{R}}_{i+n}^{-1} \mathbf{v}_t$$

In a sidelooking configuration, the clutter covariance matrix is range independent and can then be estimated from the secondary range cells. This property is however no longer true in another configuration.

2.2 Geometry of the NSL configuration

Figure 1 represents the considered system [1]. The radar antenna is positioned on an airborne platform at the altitude h and move with constant velocity $\mathbf{v}_a$. The ground clutter is split in rings of constant range R_c from the radar which are split themselves in N_c patches (here N_c = 180). Each clutter patch is described by its azimuth ϕ_c and its elevation θ_c. In the non sidelooking configuration, the platform velocity vector $\mathbf{v}_a$ is not aligned with the radar antenna axis involving a crab angle, ϕ_a. This configuration illustrates the majority of the practical cases, as for example, radars using rotating antenna, forward-looking airborne radars, etc. Also when side-mounted antenna are used, an aircraft crab is used to mitigate the wind effects [1].

The clutter spatial frequency and the normalized Doppler can then be written

$$\vartheta_c = \frac{d \cdot cos(\theta_c)}{\lambda} sin(\phi_c) \tag{5}$$

and

$$\varpi_c = \frac{2 v_a T_r}{\lambda} cos(\alpha)$$

respectively, where d is the inter-element spacing, λ is the radar wavelength and T_r is the PRI. Let α be the cone angle

$$cos(\alpha) = cos(\theta_c)\, sin(\phi_c + \phi_a) \tag{6}$$

$cos(\alpha)$ is the direction cosine between the x-axis and the unit vector pointing from R to the clutter scatterer S. We obtain

$$sin(\phi_c) = \frac{cos(\phi_a) \cdot cos(\alpha)}{cos(\theta_c)} \pm \gamma \tag{7}$$

where

$$\gamma = \sqrt{\left(\frac{cos(\alpha)}{cos(\theta_c)}\right)^2 cos^2(\phi_a) - \left(\frac{cos(\alpha)}{cos(\theta_c)}\right)^2 + sin^2(\phi_a)}$$

When using $sin(\theta_c) = \frac{h}{Rc}$ and (5) , (7) gives

$$\vartheta_c = \frac{d}{\lambda}\left(cos(\alpha)\, cos(\phi_a) \pm sin(\phi_a) \sqrt{1 - \left(\frac{h}{Rc}\right)^2 - cos^2(\alpha)}\right) \tag{8}$$

Furthermore the normalized Doppler frequency is

$$\varpi_c = \frac{d}{\lambda} cos(\alpha) \tag{9}$$

With (6) and (9), (8) gives the relation which links the clutter spatial frequency and the normalized Doppler

$$\vartheta_c = \varpi_c cos(\phi_a) \pm \frac{1}{2} sin(\phi_a) \sqrt{1 - \left(\frac{h}{Rc}\right)^2 - 4\varpi_c^2} \tag{10}$$

It appears from (10) that, in the sidelooking configuration, $\phi_a = 0^o$, the relation between the Doppler and the spatial frequency is independent of the range (Rc). In the non sidelooking configuration, however, a range dependency is observed. Consequently, the interference plus noise space time covariance matrix is also range dependent. This is illustrated in Figure 2 where the clutter ridges, which represent the space-time repartition of the clutter power, are composed of a set of ellipses for different ranges R_c instead of being a straight line independent of R_c.

This then implies a kind of non-stationarity of the data so that the classical estimator (4) of the clutter covariance matrix is no longer valid. Several methods of compensation ([2] and the reference within) have been proposed in the literature but they either are too complex or require the knowledge of the radar parameters. We investigate in the following section an alternative approach of the problem.

3. RANGE RECURSIVE STAP ALGORITHMS

Adaptive-recursive algorithms have been used for a long time in many areas of signal processing such as filtering, spectral analysis, array processing, prediction, etc. and in many applications such as channel equalization, noise cancellation, speech coding,etc. They consist in recursively updating a weight vector at time k from the weights vector obtained at time $k-1$ and by taking account of the current snapshot. These algorithms generally involve less computational operations than their block counterparts and are known to be able to track some kind of non-stationarity of the data. Also, we here propose to apply some adaptive recursive subspace-based algorithms already tested in array processing and spectral analysis [3], [4], [5] and [7] in order to reduce the computational burden, to the range dependent above mentioned STAP problem. In this section, we briefly recall the key idea of each considered algorithm and the resulting code of it.

3.1 PAST algorithm

For the PAST (Projection Approximation Subspace Tracking) algorithm [3], a basis of the interference subspace is obtained as the solution of the unconstrained minimization problem :

$$J(\mathbf{W}) = \sum_{k=1}^{t} \beta^{t-k} \left\| \mathbf{x}(i) - \mathbf{W}(t)\mathbf{W}(t)^H \mathbf{x}(i) \right\|^2 \tag{11}$$

where $\mathbf{x}$ is the observed data vector and $\mathbf{W}$ is the estimated interference subspace basis and β a forgetting factor, $0 \leq \beta < 1$. Using the following approximation $\mathbf{W}(t)^H \mathbf{x}(i) \approx \mathbf{W}(i-1)^H \mathbf{x}(i)$ (11) is reduced to the exponentially weighted least square minimization:

$$J'(\mathbf{W}(t)) = \sum_{i=1}^{t} \beta^{t-i} \left\| \mathbf{x}(i) - \mathbf{W}(t)\mathbf{y}(i) \right\|^2$$

With $\mathbf{y}(i) = \mathbf{W}(i-1)^H \mathbf{x}(i)$ this cost function has a global minimum which yields a non orthonormal basis of the interference subspace and which may be attained by a RLS adaptive algorithm given in table 1.

3.2 OPAST algorithm

The Orthogonal Projection Approximation Subspace Tracking (OPAST) algorithm [4] is an orthonormalized version which avoids the complex Gram-Schmidt orthonormalization and yields the algorithm of table 1.

3.3 API and FAPI algorithms

The Approximated Power Iteration (API) and Fast Approximated Power Iteration (FAPI) algorithms [5] derive from the power Method [6]. A less restrictive approximation than for PAST is used. Indeed it concerns the projection on the estimated subspace instead of the estimated subspace itself:

$$\mathbf{W}(i)\mathbf{W}(i)^H \approx \mathbf{W}(i-1)\mathbf{W}(i-1)^H$$

The obtained subspace is found to be orthonormalized. The FAPI algorithm is a fast implementation of API (see [5]). API and FAPI codes are exhibited in table 2.

3.4 NIC algorithm

The Novel Information Criterion (NIC) algorithm [7] consists in maximizing

$$J(\mathbf{W}) = \frac{1}{2}\left(tr\left\{log\left(\mathbf{W}^H\mathbf{R}_{xx}\mathbf{W}\right)\right\} - tr\left\{\mathbf{W}^H\mathbf{W}\right\}\right)$$

where $\mathbf{R}_{xx} = E\left\{\mathbf{x}\mathbf{x}^H\right\}$. This criterion presents a single global maximum $\frac{1}{2}\sum_{i=1}^{n} log(\lambda_i - n)$ where $\lambda_1, \ldots, \lambda_n$ are the eigenvalues of the interference subspace. The corresponding RLS algorithm is given in table 3.

3.5 remark

The above-mentioned algorithms have been selected among a wide class of linear complexity subspace-based algorithm for their good behavior in a previous work on array processing [9]. As it can be viewed on tables 1, 2, 3, the complexity burden is $O(MN)$ instead of $O((MN)^3)$ for SMI or eigencanceller. To run these algorithms, the rank of the clutter space time covariance matrix is supposed to be known. In a sidelooking configuration, according to Brennan's rule [1] it is equal to $N + (M-1)$. In a non sidelooking case, this rank is about doubled [1].

4. SIMULATION RESULTS

We here transpose the time recursive above-mentioned algorithms to range recursive STAP in order to show whether they are capable of compensating some range dependence (some non stationarity) of the data. We discuss the performance of these algorithms in terms of their SINR loss defined as follows.

$$SINRloss = \frac{\sigma^2 \cdot \left|\mathbf{w}^H\mathbf{v}_t\right|^2}{NM \cdot \mathbf{w}^H\mathbf{R}_{i+n}\mathbf{w}}$$

where $\mathbf{w}$ is the weight vector calculated (according to each algorithm). The optimum SINR loss is

$$SINRloss_{opt} = \frac{\sigma^2 \cdot \mathbf{v}_t^H\mathbf{R}_{i+n}^{-1}\mathbf{v}_t}{NM}$$

For the analysis, a pulsed Doppler airborne monostatic radar in forward looking configuration $\phi_a = 90^o$ is considered. The platform has an altitude of 9 km and is moving with a velocity of 100 m/s. The operating frequency of the radar is 10 GHz with a PRF of 13 kHz. The radar bandwidth is 100 MHz. The array is composed of 12 uniformly spaced elements. 10 pulses are transmitted during a CPI.

Figures 3 to 6 show a slice of SINR loss at spatial frequency 0 degree versus the normalized Doppler frequency employing 240 training data (it correspond to 2NM) for the figures 3 and 4 and 480 (4NM) for the figures 5 and 6. The secondary data are chosen before the range test cell. The results are averaging over 20 Monte Carlo trials. In the first and third simulations, R_c is equal to 9000 m. It involves a nearly constant gap between the clutter ridges and thus the non stationarity can be qualified of severe. In the two others, it is set to 15000 m; the gap between the clutter ridges decreases over the simulation. Thus the non stationarity is lower. The range-recursive algorithms outperform the SMI algorithm in any case. The different tested algorithms are globally equivalent. However we can discuss of their relative merits. We can differentiate the performances of these algorithms according to the degree of non stationarity: in case of a severe non stationarity (figures 3 and 4), PAST and OPAST algorithms are outperformed by NIC, API and FAPI algorithms. On the contrary, in case of a light stationarity (figures 5 and 6), NIC algorithm is outperformed by the others. In conclusion, within these algorithms FAPI and API algorithms outperformed the others. The forgetting factor is chosen to be ideal for these non stationarities equal to 0.8. More generally the range-recursive algorithms showed good performance when the range dependence does not decrease too fast. That's why the ideal case is a good range resolution (between 1 and 3m). These algorithms must thus be used in case of non sidelooking configuration with any crab angle and for X-band or C-band radars.

Table 1 PAST and OPAST Algorithms

Initialization : $\mathbf{W}(0) \leftarrow \mathbf{I}_{M\times N}$, $\mathbf{Z}(0) \leftarrow \mathbf{I}_{N\times N}$

for $k = 1$ to Nbr snapshot **do**

PAST main section

$\mathbf{y}(k) = \mathbf{W}(k-1)^H \cdot \mathbf{x}(k)$

$\mathbf{h}(k) = \mathbf{Z}(k-1) \cdot \mathbf{y}(k)$

$\mathbf{g}(k) = \frac{\mathbf{h}(k)}{\beta + \mathbf{y}^H(k)\cdot\mathbf{h}(k)}$

$\mathbf{e}(k) = \mathbf{x}(k) - \mathbf{W}(k-1)\cdot\mathbf{y}(k)$

PAST secondary section

$\mathbf{Z}(k) = \frac{1}{\beta}\cdot(\mathbf{Z}(k-1) - \mathbf{g}(k)\cdot\mathbf{y}(k)^H\cdot\mathbf{Z}(k-1))$

$\mathbf{W}(k) = \mathbf{W}(k-1) + \mathbf{e}(k)\cdot\mathbf{g}(k)^H$

OPAST main section

$\gamma(k) = \frac{1}{\beta + \mathbf{y}(k)^H\cdot\mathbf{h}(k)}$

$\mathbf{Z}(k) = \frac{1}{\beta}\cdot\left(\mathbf{Z}(k-1) - \mathbf{g}(k)\cdot\mathbf{y}(k)^H\cdot\mathbf{Z}(k-1)\right)$

$\tau(k) = \frac{\beta^2}{\|\mathbf{h}(k)\|^2}\cdot\left(\frac{1}{\sqrt{\beta^2 + \|\gamma(k)\cdot\mathbf{e}(k)\|^2\|\mathbf{h}(k)\|^2}} - 1\right)$

$\mathbf{p}'(k) = \frac{1}{\beta}\tau(k)\mathbf{W}(k-1)\mathbf{h}(k) + \left(\beta^2 + \tau(k)\|\mathbf{h}(k)\|^2\right)\gamma(k)\mathbf{e}(k)$

$\mathbf{W}(k) = \mathbf{W}(k-1) + \frac{1}{\beta}\mathbf{p}'(k)\cdot\mathbf{h}(k)^H$

end for

Table 2 API and FAPI Algorithms

Initialization : $\mathbf{W}(0) \leftarrow \mathbf{I}_{M\times N}$, $\mathbf{Z}(0) \leftarrow \mathbf{I}_{N\times N}$

for $k = 1$ to Nbr snapshot **do**

PAST main section (see Algorithm 1)

API main section

$\mathbf{\Theta}(k) = \frac{1}{\sqrt{\mathbf{I}_{N\times N} + \|\mathbf{e}(k)\|^2\mathbf{g}(k)\mathbf{g}(k)^H}}$

$\mathbf{Z}(k) = \frac{1}{\beta}\cdot(\mathbf{I} - \mathbf{g}(k)\cdot\mathbf{y}(k)^H)\mathbf{Z}(k-1)\mathbf{\Theta}(k)^{-H}$

$\mathbf{W}(k) = \left(\mathbf{W}(k-1) + \mathbf{e}(k)\mathbf{g}(k)^H\right)\mathbf{\Theta}(k)$

FAPI main section

$\varepsilon^2(k) = \|\mathbf{x}(k)\|^2 - \|\mathbf{y}(k)\|^2$

$\tau(k) = \frac{\varepsilon^2(k)}{1 + \varepsilon^2(k)\|\mathbf{g}(k)\|^2 + \sqrt{1 + \varepsilon^2(k)\|\mathbf{g}(k)\|^2}}$

$\eta(k) = 1 - \tau(k)\|\mathbf{g}(k)\|^2$

$\mathbf{y}'(k) = \eta(k)\mathbf{y}(k) + \tau(k)\mathbf{g}(k)$

$\mathbf{h}'(k) = \mathbf{Z}(k-1)^H\mathbf{y}'(k)$

$\epsilon(k) = \frac{\tau(k)}{\eta(k)}(\mathbf{Z}(k-1)\mathbf{g}(k) - (\mathbf{h}'(k)\mathbf{g}(k))\mathbf{g}(k))$

$\mathbf{Z}(k) = \frac{1}{\beta}(\mathbf{Z}(k-1) - \mathbf{g}(k)\mathbf{h}'(k)^H + \epsilon(k)\mathbf{g}(k)^H)$

$\mathbf{e}'(k) = \eta(k)\mathbf{x}(k) - \mathbf{W}(t-1)\mathbf{y}'(k)$

$\mathbf{W}(k) = \mathbf{W}(k-1) + \mathbf{e}'(k)\cdot\mathbf{g}(k)^H$

end for

5. CONCLUSION AND FUTURE WORK

The non sidelooking configuration involves different kinds of problem including the range dependency. In this paper, we showed that we can mitigate this problem by using range recursive algorithms which can estimate recursively the weights of the clutter rejection filter and thus track this non stationarity through the medium of the forgetting factor. We have presented the good performance of a number of adaptive recursive subspace-based algorithms of linear complexity under simulation of a case of a very severe non stationarity and in comparison with the SMI algorithm and with the

Table 3 NIC Algorithm

Initialization : $\mathbf{W}(0) \leftarrow \mathbf{I}_{M\times N}$, δ small positive integer ,
$\mathbf{Z}(0) \leftarrow \delta \cdot \mathbf{I}_{N\times N}$, $\tilde{\mathbf{W}}(0) \leftarrow$ nul matrix

for $k = 1$ to Nbr snapshot **do**

$\mathbf{y}(k) = \mathbf{W}(k-1)^H \cdot \mathbf{x}(k)$

$\mathbf{h}(k) = \mathbf{Z}(k-1) \cdot \mathbf{y}(k)$

$\mathbf{g}(k) = \frac{\mathbf{h}(k)}{\beta + \mathbf{y}^H(k) \cdot \mathbf{h}(k)}$

$\mathbf{Z}(k) = \frac{1}{\beta} \cdot (\mathbf{Z}(k-1) - \mathbf{g}(k) \cdot \mathbf{y}(k)^H \cdot \mathbf{Z}(k-1))$

$\mathbf{e}(k) = \mathbf{x}(k) - \tilde{\mathbf{W}}(k-1)^H \cdot \mathbf{y}(k)$

$\tilde{\mathbf{W}}(k) = \tilde{\mathbf{W}}(k-1) + \mathbf{e}(k) \cdot \mathbf{g}(k)^H$

$\mathbf{W}(k) = (1-\eta) \cdot \mathbf{W}(k-1) + \eta \cdot \tilde{\mathbf{W}}(k)$

end for

optimal filter. Furthermore, they present a very low computational complexity. That's why these algorithms can be considered as an economical approach in comparison with the other techniques. Our purpose was here to test the capability and the limits of these range recursive algorithms to track this form of non stationarity without the help of compensation method. The future investigations will be the use of a variable forgetting factor which can be adapted at each iteration to the non stationarity degree and the use of compensation methods to further outperforming these results. We are also studying a comparison of the proposed algorithms with compensation methods as Lapierre algorithms [2] and with other methods as the linear prediction of the inverse clutter covariance matrix [10]. The bistatic configuration is also under consideration.

REFERENCES

[1] J. Ward, "Space-Time Adaptive Processing for airborne radar," *Technical Report 1015*, Lincoln Laboratory MIT, Dec. 1994.

[2] F. Lapierre, "Registration-based Range-dependence compensation in Airborne Bistatic Radar STAP", *PhD Thesis*, Liège, 2005.

[3] B. Yang, "Projection Approximation Subspace Tracking," *IEEE Transactions on Signal Processing*, vol. 43, pp. 95–107, Jan. 1995.

[4] K. Abed-Meraim A. Chkeif and Y. Hua, "Fast Orthonormal PAST Algorithm," *IEEE Signal Processing Letters*, vol. 7, pp. 60–62, Mar. 2000.

[5] R. Badeau, B. David, and G. Richard, "Fast approximated power iteration subspace tracking," *IEEE Transactions on Signal Processing*, vol. 53, pp. 2931–2941, Aug. 2005.

[6] Y. Hua, Y. Xiang, T. Chen, K. Abed-Meraim, and Y. Miao, "A new look at the power method for fast subspace tracking", *IEEE Digital Signal Processing*, Oct. 1999.

[7] Y. Miao and Y. Hua, "Fast Subspace Tracking and Neural Network Learning by a Novel Information Criterion," *IEEE Transactions on Signal Processing*, vol. 46, pp. 1967–1979, Jul. 1998.

[8] H. Belkacemi and S. Marcos, "Fast iterative subspace algorithms for airborne STAP radar", *Journal of Signal Processing Special Issue on Multisensor Processing for Signal extraction and applications*, 2006, article ID 37296.

[9] S. Beau and S. Marcos, " Performances et capacité de poursuite d'algorithmes adaptatifs à complexité linéaire basés sur des méthodes de sous-espaces," *Internal Report*, CNRS, Supelec, Nov. 2006.

[10] C.H. Lim and B. Mulgrew, " Prediction of Inverse Covariance Matrix (PICM) Sequences for STAP," *IEEE Signal Processing letters*, vol. 13, pp. 236–239, Apr. 2006.

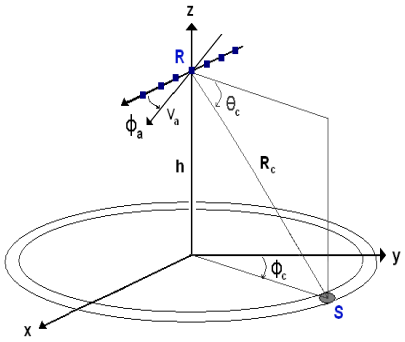

Figure 1: Geometry of the monostatic non sidelooking configuration

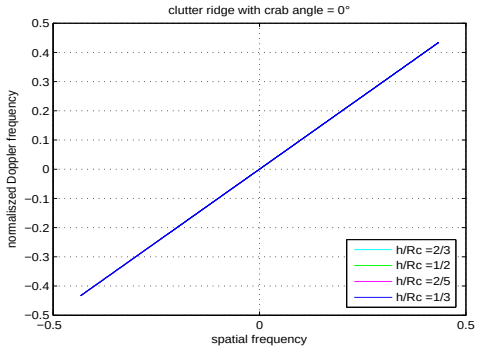

(a)

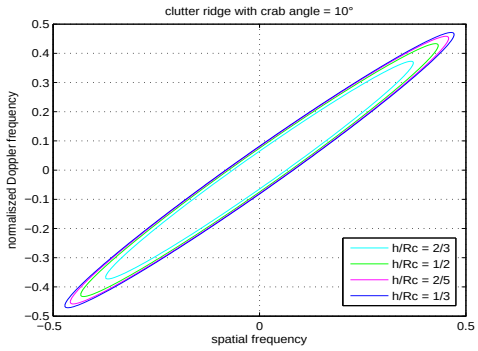

(b)

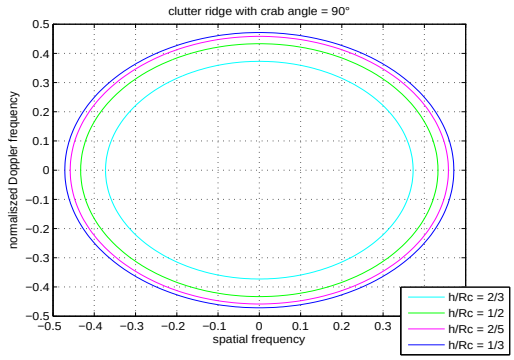

(c)

Figure 2: Examples of clutter ridges. No velocity misalignment (a) ; velocity misalignment of 10^o (b), velocity misalignment of 90^o (c)

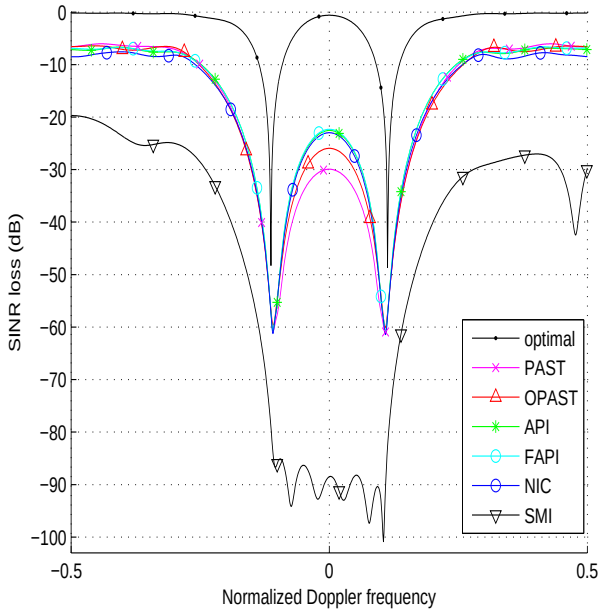

Figure 3: Slice of SINR loss at spatial frequency $= 0^o$ with 240 secondary range cells and $R_c = 9000m$ (Monte Carlo simulations over 20 simulations)

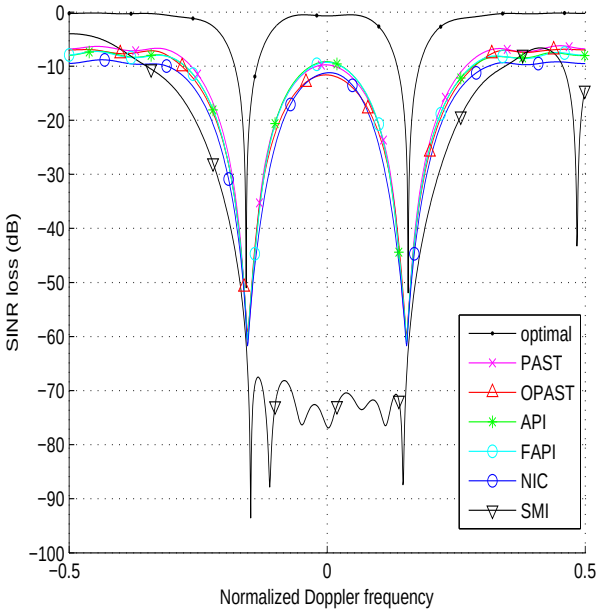

Figure 5: Slice of SINR loss at spatial frequency $= 0^o$ with 480 secondary range cells and $R_c = 9000m$ (Monte Carlo simulations over 20 simulations)

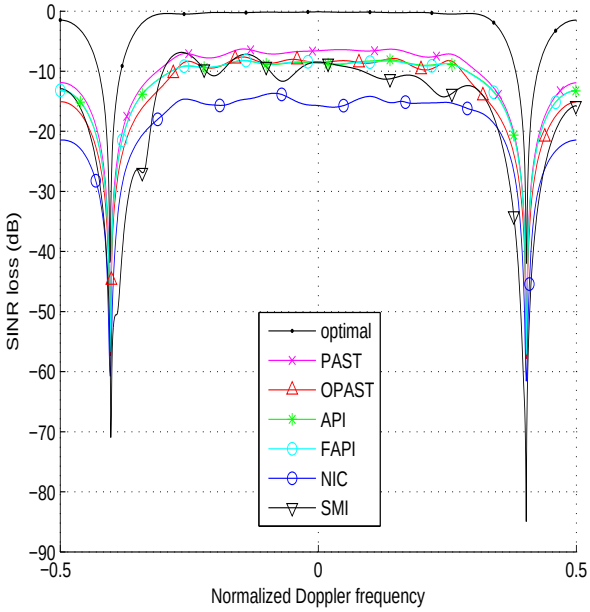

Figure 4: Slice of SINR loss at spatial frequency $= 0^o$ with 240 secondary range cells and $R_c = 15000m$ (Monte Carlo simulations over 20 simulations)

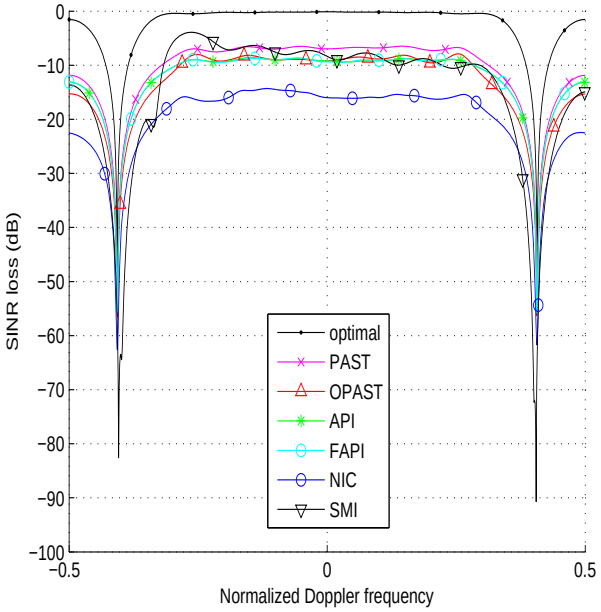

Figure 6: Slice of SINR loss at spatial frequency $= 0^o$ with 480 secondary range cells and $R_c = 15000m$ (Monte Carlo simulations over 20 simulations)